1-20-2012

Pressure-overload-induced subcellular relocalization/oxidation of soluble guanylyl cyclase in the heart modulates enzyme stimulation.

Emily J Tsai
Temple University School of Medicine; Johns Hopkins University

Yuchuan Liu
Temple University School of Medicine

Norimichi Koitabashi
Johns Hopkins University

Djahida Bedja
Johns Hopkins University

Thomas Danner
Johns Hopkins University

Circulation Research
JOURNAL OF THE AMERICAN HEART ASSOCIATION

Pressure-Overload–Induced Subcellular Relocalization/Oxidation of Soluble Guanylyl Cyclase in the Heart Modulates Enzyme Stimulation

Emily J. Tsai, Yuchuan Liu, Norimichi Koitabashi, Djahida Bedja, Thomas Danner, Jean-Francois Jasmin, Michael P. Lisanti, Andreas Friebe, Eiki Takimoto and David A. Kass

Circ Res. 2012;110:295-303; originally published online November 17, 2011;
doi: 10.1161/CIRCRESAHA.111.259242
Circulation Research is published by the American Heart Association, 7272 Greenville Avenue, Dallas, TX 75231

Print ISSN: 0009-7330. Online ISSN: 1524-4571

Pressure-Overload–Induced Subcellular Relocalization/Oxidation of Soluble Guanylyl Cyclase in the Heart Modulates Enzyme Stimulation

Emily J. Tsai, Yuchuan Liu, Norimichi Koitabashi, Djahida Bedja, Thomas Danner, Jean-Francois Jasmin, Michael P. Lisanti, Andreas Friebe, Eiki Takimoto, David A. Kass

Rationale: **Soluble guanylyl cyclase (sGC) generates cyclic guanosine monophosphate (cGMP) upon activation by nitric oxide (NO). Cardiac NO–sGC-cGMP signaling blunts cardiac stress responses, including pressure-overload–induced hypertrophy. The latter itself depresses signaling through this pathway by reducing NO generation and enhancing cGMP hydrolysis.**

Objective: **We tested the hypothesis that the sGC response to NO also declines with pressure-overload stress and assessed the role of heme-oxidation and altered intracellular compartmentation of sGC as potential mechanisms.**

Methods and Results: **C57BL/6 mice subjected to transverse aortic constriction (TAC) developed cardiac hypertrophy and dysfunction. NO-stimulated sGC activity was markedly depressed, whereas NO- and heme-independent sGC activation by BAY 60–2770 was preserved. Total sGCα_1 and β_1 expression were unchanged by TAC; however, sGCβ_1 subunits shifted out of caveolin-enriched microdomains. NO-stimulated sGC activity was 2- to 3-fold greater in Cav3-containing lipid raft versus nonlipid raft domains in control and 6-fold greater after TAC. In contrast, BAY 60–2770 responses were >10 fold higher in non-Cav3 domains with and without TAC, declining about 60% after TAC within each compartment. Mice genetically lacking Cav3 had reduced NO- and BAY-stimulated sGC activity in microdomains containing Cav3 for controls but no change within non–Cav3-enriched domains.**

Conclusions: **Pressure overload depresses NO/heme-dependent sGC activation in the heart, consistent with enhanced oxidation. The data reveal a novel additional mechanism for reduced NO-coupled sGC activity related to dynamic shifts in membrane microdomain localization, with Cav3-microdomains protecting sGC from heme-oxidation and facilitating NO responsiveness. Translocation of sGC out of this domain favors sGC oxidation and contributes to depressed NO-stimulated sGC activity. (*Circ Res*. 2012;110:295-303.)**

Key Words: hypertrophy ■ soluble guanylyl cyclase ■ caveolae ■ signaling ■ cardiomyocyte

Heart failure affects more than 6 million patients in the United States alone, and its prevalence continues to rise despite recent diagnostic and therapeutic advances. A leading risk factor for the disease is chronic pressure overload due to arterial hypertension, which afflicts nearly a third of the world's population. Such sustained stress often induces pathological hypertrophy of the chamber wall and can lead to depressed function and electric instability. Current treatment reduces the pressure load and suppresses neurohormones that contribute to maladaptive remodeling. However, clinical outcome remains poor, and as a consequence, novel approaches to leverage intrinsic negative modulators of hypertrophy are garnering increasing attention.

One such pathway involves the second messenger cyclic guanosine monophosphate (cGMP).[1–3] Cyclic GMP is generated by either the particulate guanylyl cyclase (pGC) linked to the natriuretic peptide receptor, or "soluble" GC (sGC), activated by nitric oxide (NO). Once generated, cGMP can modulate cardiomyocyte function by interacting with phosphodiesterases (PDEs) that regulate cAMP and its associated pathways, or by activating its primary target kinase, protein kinase G (PKG, also called cGK-1). Cyclic GMP-PKG

Original received October 20, 2011; revision received November 5, 2011; accepted November 8, 2011. In October 2011, the average time from submission to first decision for all original research papers submitted to *Circulation Research* was 15 days.

From the Section in Cardiology, Department of Medicine, Temple University School of Medicine, Philadelphia, PA (E.J.T.); Cardiovascular Research Center, Temple University School of Medicine, Philadelphia, PA (E.J.T., Y.L.); the Division of Cardiology, Department of Medicine, Johns Hopkins University Medical Institutions, Baltimore, MD (E.J.T., N.K., T.D., E.T.); the Department of Comparative Medicine and Comparative Pathology, Johns Hopkins University Medical Institutions, Baltimore, MD (D.B.); the Department of Stem Cell Biology and Regenerative Medicine, Thomas Jefferson University, Philadelphia, PA (J.-F.J., M.P.L.); the Department of Cancer Biology, Thomas Jefferson University, Philadelphia, PA (M.P.L.); and Physiologisches Institut I, Universität Würzburg, Würzburg, Germany (A.F.).

Correspondence to David A. Kass, MD, Division of Cardiology, Johns Hopkins Medical Institutions, 720 Rutland Ave, Ross 858, Baltimore, MD 21205 (E-mail dkass@jhmi.edu); or Emily J. Tsai, MD, Cardiovascular Research Center, Temple University School of Medicine, 3500 N Broad St, MERB 1047, Philadelphia, PA 19140. (E-mail emily.tsai@tuhs.temple.edu).

Circulation Research **is available at http://circres.ahajournals.org** **DOI: 10.1161/CIRCRESAHA.111.259242**

Non-standard Abbreviations and Acronyms	
Cav3	caveolin-3
cAMP	cyclic adenosine monophosphate
cGMP	cyclic guanosine monophosphate
cGK	cyclic GMP-dependent protein kinase
DEA/NO	diethylamine NONOate
FS	fractional shortening
IBMX	3-isobutyl-1-methylxanthine
KO	knockout
LR	lipid raft
LV	left ventricle
NLR	nonlipid raft
NO	nitric oxide
NOS3	endothelial NO synthase
ODQ	1H-[1,2,4] oxadiazolo[4,3-a] quinox-alin1-one
PDE	phosphodiesterase
PKG	protein kinase G
pGC	particulate guanylyl cyclase
sGC	soluble guanylyl cyclase
TAC	transverse aortic constriction
WT	wild-type

activation plays a key role in modulating vascular tone and confers antifibrotic effects. Newer studies support a potent role in suppressing cardiomyocyte pathobiology, including blunting in vivo pressure-overload–induced hypertrophy and protecting against ischemia-reperfusion injury and myocyte apoptosis.[4–11] However, in chronic pressure overload, myocardial NO synthesis and secondary signaling through cGMP is itself depressed[9,12–16] probably contributing to the pathophysiology. The latter appears related in part to an increase in cGMP hydrolysis by targeting phosphodiesterases such as PDE1 and PDE5.[9,15,16]

Another key component of this signaling pathway is sGC itself, yet no prior studies have examined its activity or potential modulators of activity in cardiac hypertrophy. Although sGC-derived cGMP is mostly thought to accumulate in the cytosol, some NO-stimulated cGMP production is detectable at the plasma membrane.[17–19] In endothelial cells, endothelial NO synthase (NOS3) and PKG colocalize with caveolin, an integral membrane scaffolding protein that compartmentalizes and concentrates signaling molecules within specialized regions of the plasma membrane. This has suggested that caveolae, small (50–100 nm) flask-like lipid- and protein-rich invaginations of the plasma membrane, may serve as microdomains for optimized NO-sGC-cGMP signaling.[20] In this regard, sGC has been found at the plasma membrane in rat neurons, rat vascular endothelial cells, human and rat skeletal myocytes, rat cardiac myocytes, and human platelets.[19–23] The importance of this localization and whether it is impacted by heart disease to contribute to altered sGC function is unknown.

The present study tested the hypothesis that sustained pressure overload depresses NO-stimulated sGC activation and explored mechanisms for such change including loss of NO- and heme-dependent activity and shifts in microdomain localization. We reveal novel evidence for both, revealing a shift of sGC out of caveolae-enriched membrane microdomains after sustained pressure overload, with enhanced sGC oxidation, and net depression of NO-stimulated cGMP generation.

Methods

Full details can be found in the Methods section of the Online Data Supplement at http://circres.ahajournals.org.

Animal Model

Male C57BL/6 mice (age, 9–12 weeks, Jackson Labs, Bar Harbor, ME) were used. Pressure overload was produced by transverse aortic constriction (TAC) as previously described.[9] Left ventricular (LV) cardiac tissue of caveolin-3 null[24] (Cav3 KO background strain C57BL/6 mice) and littermate controls (wild-type [WT]) mice were provided by JF Jasmin (Thomas Jefferson University).[25] All animals received humane care according to National Institutes of Health guidelines, and all animal protocols were approved by the respective IACUCs of Johns Hopkins University and Temple University.

Physiological Study

Cardiac function was assessed in conscious and isoflurane-anesthetized mice by transthoracic, 2D, M-mode echocardiography (Acuson Sequoia C256, Siemens at Johns Hopkins and Vevo660, Visual Sonics at Temple) with a 15-MHz linear-array transducer. M-mode LV end-systolic and end-diastolic dimensions were averaged from 3 to 5 beats. LV percent fractional shortening (FS) and mass were calculated as described previously.[9]

Immunofluorescent and Confocal Microscopy

Immunohistochemical analysis was performed on paraffin-embedded, 10% formaldehyde gravity-perfused LV tissue. LV tissue slices were imaged with a Nikon C-1 PLUS confocal microscope system.

Cell Fractionation

Protein was prepared from snap-frozen heart tissue, and membrane-cytosol fractionation was performed as previously described.[9,26]

Isolation of Caveolin-Enriched Lipid Raft Fraction

Caveolin-enriched lipid raft fractions ($Cav3^+$LR) were prepared from freshly harvested and snap-frozen LV tissue, using a discontinuous 35–5% sucrose density gradient ultracentrifugation method as previously described,[27] with some modifications.

Western Blot Analysis

Protein extracts from LV tissue homogenate and above mentioned subfractions were run on SDS-PAGE gels and transferred to nitrocellulose membranes. Immunoblot analysis was performed using primary antibody probes as detailed in the Online Data Supplement.

sGC Activity and cGMP Measurement

Baseline and agonist-stimulated cGMP levels of total LV, $Cav3^+$LR, and nonenriched fractions (NLR) from Sham, TAC, WT, and Cav3 KO hearts were measured by direct cGMP ELISA kit from New East Biosciences (Malvern, PA).

Statistical Analysis

All values are expressed as mean±SEM. Statistical analyses were performed using Student *t* test, 1-way ANOVA followed by Tukey test when comparing multiple groups, or 2-way ANOVA when determining interaction of conditions. For data sets with unequal variances, a Welch *t* test was used. Statistical significance was defined as $P<0.05$.

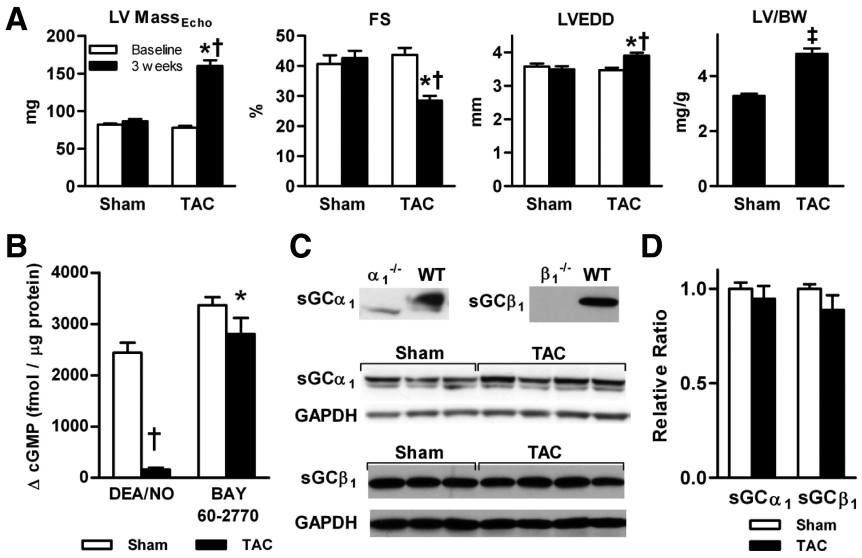

Figure 1. Hypertrophied hearts have reduced sGC activity despite unchanged expression levels of sGCα_1 and β_1 subunits. A, LV mass, fractional shortening, and LV end-diastolic diameter of sham (n=31) and TAC (n=48) mice at baseline and 3 weeks after surgery as measured by echocardiography. LV mass to body weight ratio: *$P<0.0002$ versus baseline; †$P<0.002$ versus respective sham; ‡$P<0.00001$ versus sham. **B**, sGC activity of total protein from sham and TAC hearts in response to NO-donor DEA/NO 1 μmol/L (n=15 for sham, 14 for TAC) and NO- and heme-independent sGC activator BAY 60–2770 0.1 mmol/L (n=7 for sham, 6 for TAC). *$P<0.01$ versus respective DEA/NO; †$P<0.00001$ versus respective sham. **C** and **D**, Western immunoblots and normalized densitometry analysis of total sGCα_1 and sGCβ_1 expression in sham (n=9 for α_1, n=6 for β_1) and TAC (n=10 for α_1, n=6 for β_1). Data are mean±SEM.

Results

Cardiac sGC Activity Declines in Hypertrophied Myocardium Despite Preserved Overall Myocardial sGCα_1 and β_1 Expression

C57BL/6J mice subjected to 3 weeks of transverse aortic constriction (TAC)[9] developed LV hypertrophy, systolic dysfunction, and dilatation (Figure 1A), as previously reported.[9,28] The capacity to stimulate myocardial sGC was assessed by the change in cGMP generation before and after exposure to NO, using the NO-donor diethylamine NONOate (DEA/NO, 1 μmol/L) in the presence of the broad PDE inhibitor IBMX (3-isobutyl-1-methylxanthine, 0.75mmol/L). Mean baseline cGMP was ≈40% lower after TAC (Table 1), but this disparity was markedly amplified on DEA/NO stimulation (Figure 1B), with a 10-fold higher NO-stimulated response in sham versus TAC. As a control, tissue extracts were pretreated with the selective, irreversible, heme-site sGC inhibitor 1H-[1,2,4] oxadiazolo[4,3-a]quinoxalin1-one (ODQ at 10, 30, and 90 μmol/L), which blocked NO-stimulated cGMP by 80–90% (Online Figure I).

Because TAC induces myocardial oxidative stress[13] and oxidation of the sGC heme moiety suppresses its NO-stimulated activity,[29] we tested whether this may have contributed to the response in TAC hearts. sGC was activated in an NO- and heme-independent manner by BAY 60–2770 (0.1μmol/L)[30] in the presence of IBMX (Figure 1B). BAY 60–2770 induced similar cGMP production as with DEA/NO in sham controls but also triggered this response in TAC heart lysate. This indicates that the depressed DEA/NO response in TAC probably is not related to reduced sGC expression per se but rather to sGC heme-oxidation.

To confirm whether sGC expression was in fact unaltered by TAC, immunoblots were performed using specific column-purified antibodies to the α_1-subunit[31] or β_1-subunit. Functional sGC exists as a heterodimer with an α (73–82 kDa) and β subunit (70 kDa), the latter reportedly expressed diffusely within cells and necessary for NO responsiveness.[32,33] The $\alpha_1\beta_1$ isoform is the most ubiquitously expressed across tissue types and the only isoform in myocardium.[34] Negative controls were provided using heart tissue from mice genetically lacking either sGCα_1[35] or sGCβ_1[31] (Figure 1C). We found expression of sGC α_1- and β_1-subunits, relative to GAPDH, was unaltered by TAC (Figure 1D).

Table 1. Baseline cGMP Levels

	Sham	TAC	*P*
Total	170.1±24.8	102.8±8.1	0.02
Cav3$^+$LR	1220.2±209.6	754.4±86.8	0.08
NLR	199.4±34.1*	297.8±88.7*	0.3

Values are mean±SEM (fmol/μg).
*$P<0.05$ on paired Student *t* test versus respective Cav3$^+$LR.

Myocardial sGC Localizes in Cytosolic and Membrane Compartments

Given unchanged protein expression, we next questioned whether TAC alters the subcellular distribution of either or both sGC subunits. LV extracts from sham and TAC mice were subfractionated into cytosol and membrane compartments and analyzed by immunoblot (Figure 2A).[36] GAPDH and Cav3 served as markers for cytosol and membrane fractions, respectively. In both sham and TAC hearts, the total cytosol-to-membrane ratio of sGCα_1 expression was similar, with approximately 66% in cytosol, 33% in the membrane (Figure 2B). This is consistent with prior studies performed in rat myocardium[19] and frog cardiomyocytes.[18] In contrast, sGCβ_1 distribution was slightly altered by TAC. In sham hearts, sGCβ_1 was nearly equally divided between cytosol and membrane fractions (47±3.4% in cytosol, 53±3.4% in membrane). In TAC hearts, sGCβ_1 distribution was predominantly cytosolic, with about 60% of total sGCβ_1 localized in the cytosol and 40% in the membrane fraction ($P=0.018$ versus sham).

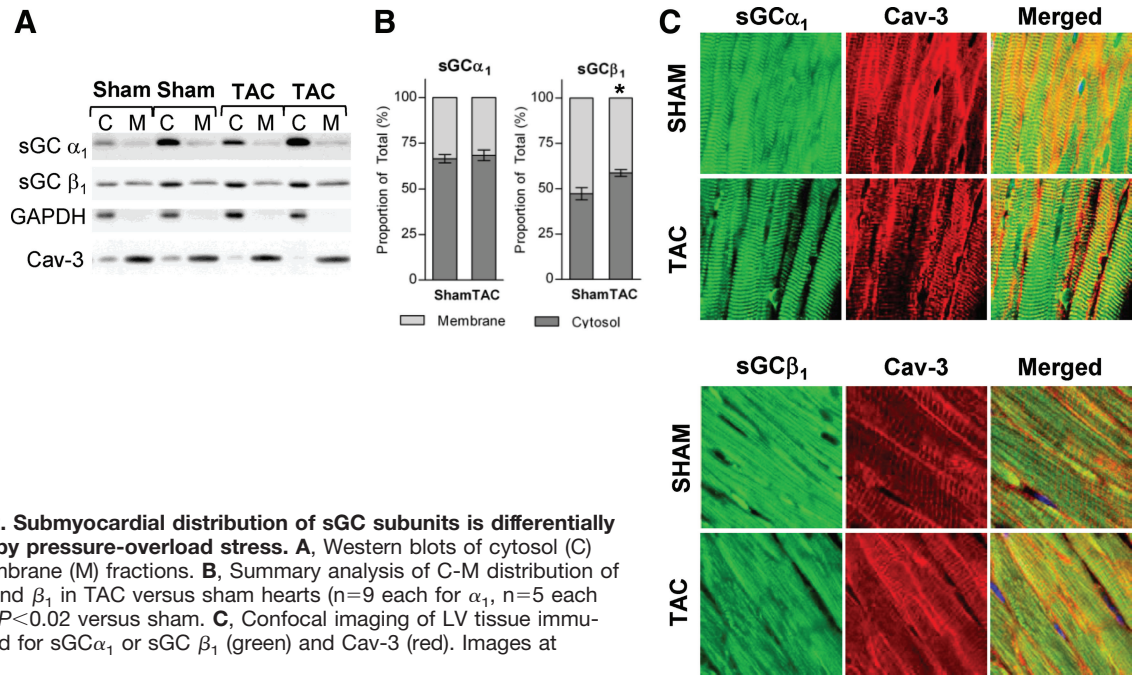

Figure 2. Submyocardial distribution of sGC subunits is differentially altered by pressure-overload stress. A, Western blots of cytosol (C) and membrane (M) fractions. **B**, Summary analysis of C-M distribution of sGCα_1 and β_1 in TAC versus sham hearts (n=9 each for α_1, n=5 each for β_1). *$P<0.02$ versus sham. **C**, Confocal imaging of LV tissue immunostained for sGCα_1 or sGC β_1 (green) and Cav-3 (red). Images at ×100.

Confocal immunohistochemistry of formaldehyde perfusion-fixed LV tissue revealed colocalization of sGCα_1 with Cav-3 in sham hearts at both plasmalemma and T-tubular membranes (Figure 2C). In TAC hearts, sGCα_1 remained present at both membrane sites though colocalization with Cav3 appeared slightly disrupted. By contrast, sGCβ_1 was distributed diffusely throughout the myocardium in a longitudinal pattern, displaying some colocalization with Cav3. This did not appear altered by TAC.

Pressure Overload Stress Alters Membrane Microdomain Localization of sGCβ_1 Subunit

To more directly examine whether sGC localization within plasma membrane compartments is altered by TAC, we determined the distribution of sGCα_1 and sGCβ_1 in microdomains of sham and TAC hearts (Figure 3). Sham and TAC LV homogenates were subjected to detergent-free, discontinuous 35–5% sucrose density gradient centrifugation to separate caveolae-enriched lipid raft microdomains (F4 and F5, Cav3$^+$LR) from nonenriched domains (F11, NLR). Each sucrose density gradient fraction was run in equal volume on SDS-PAGE electrophoresis (Figure 3B). Protein concentrations determined by Bradford assay confirmed that total protein distribution was weighted toward heavier fractions (F6 and higher) lacking Cav3 in both control and TAC hearts (Figure 3C). In sham controls, sGCα_1 and sGCβ_1 were detected in caveolae-enriched and nonenriched microdomains. In sham controls, the distribution of sGCα_1, sGCβ_1, and Cav3 across fractions revealed sGCα_1 and sGCβ_1 to be relatively higher in Cav3$^+$LR after normalizing to total protein within the respective fraction. However, in TAC hearts, the proportion of sGCβ_1 present in Cav3$^+$LR declined (Figure 3D and 3E).

Pressure-Overload Cardiac Stress Differentially Reduces NO-Induced sGC Activity in Caveolae-Enriched Lipid Raft and Nonenriched Microdomains

To test whether membrane microdomain localization of sGC influenced its functional response to NO, Cav3$^+$LR and NLR fractions were assayed for NO and BAY 60–2770–stimulated cGMP generation (Figure 4). As before, measurements were made in the presence of IBMX, so cGMP generation could be stably detected. Baseline cGMP in respective caveolae-enriched or nonenriched microdomains were similar between sham and TAC (Table 1). However, cGMP levels were ≈3-fold higher in caveolae-enriched microdomains ($P=0.01$ for sham, $P=0.04$ for TAC). More strikingly, NO-stimulated cGMP production was markedly greater in caveolae-enriched versus nonenriched fractions, and this was observed in sham and TAC similarly (note logarithmic scale). However, NO-induced sGC activity was also uniformly higher in sham Cav3$^+$LR and NLR fractions compared to corresponding domains in TAC hearts ($P<0.05$ on paired Student t test for all NLR measurements versus respective Cav3$^+$LR). In contrast to NO stimulation, the sGC response to BAY 60–2770 was >10-fold greater in NLR than Cav3$^+$LR fractions, and this held similarly for sham and TAC hearts. In NLR fractions, the BAY 60–2770 response exceeded that to DEA/NO, whereas in Cav3$^+$LR fractions, the 2 responses were similar. This pattern persisted after TAC. BAY 60–2770 activates sGC in a heme-independent manner, and this response is enhanced by heme-oxidation,[30,37] supporting greater sGC oxidation in NLR fractions, be they in sham or TAC hearts. With TAC, the concordant reduction in both NO and BAY 60–2770 responsiveness of Cav3$^+$LR fraction is consistent with a shift of sGC away from caveolae-enriched into nonenriched microdomains. Two-way ANOVA

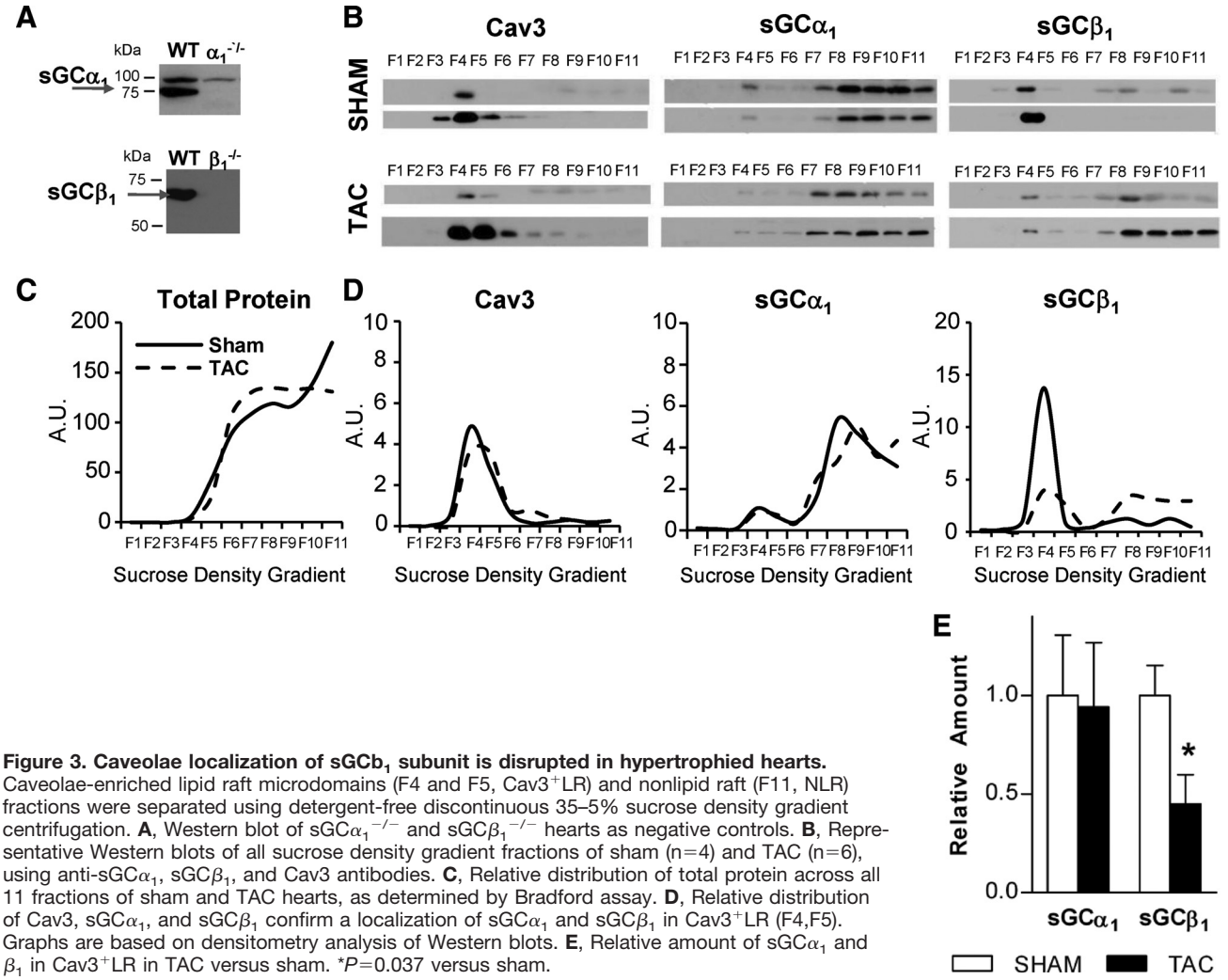

Figure 3. Caveolae localization of sGCb$_1$ subunit is disrupted in hypertrophied hearts. Caveolae-enriched lipid raft microdomains (F4 and F5, Cav3$^+$LR) and nonlipid raft (F11, NLR) fractions were separated using detergent-free discontinuous 35–5% sucrose density gradient centrifugation. **A**, Western blot of sGC$\alpha_1{}^{-/-}$ and sGC$\beta_1{}^{-/-}$ hearts as negative controls. **B**, Representative Western blots of all sucrose density gradient fractions of sham (n=4) and TAC (n=6), using anti-sGCα_1, sGCβ_1, and Cav3 antibodies. **C**, Relative distribution of total protein across all 11 fractions of sham and TAC hearts, as determined by Bradford assay. **D**, Relative distribution of Cav3, sGCα_1, and sGCβ_1 confirm a localization of sGCα_1 and sGCβ_1 in Cav3$^+$LR (F4,F5). Graphs are based on densitometry analysis of Western blots. **E**, Relative amount of sGCα_1 and β_1 in Cav3$^+$LR in TAC versus sham. *P=0.037 versus sham.

of the cGMP responses to DEA/NO in the caveolae-enriched and nonenriched microdomains of sham and TAC hearts revealed that both pressure-overload and microdomain localization affected sGC NO-responsiveness ($P<0.001$ for both), with a borderline interaction effect ($P=0.06$). This disparity is further quantified in Table 2. An increase in the BAY 60–2770–to–DEA/NO relative responses occurs with heme-oxidation. Within Cav3$^+$LR fractions, this relative response ratio was unaltered by TAC; however, it dramatically rose in NLR fractions.

Loss of Caveolin 3 Blunts sGC NO Responsiveness Specifically in Lipid Raft Fractions

To further test whether caveolae represent enhanced microdomains for NO-inducible sGC activity, we studied sGC responsiveness in hearts of caveolin-3 null (Cav3KO) mice. The model develops spontaneous mild cardiac hypertrophy by 4 months of age.[38] For whole myocardial analysis, we examined 6-month-old hearts, which had a <10% higher LV/body weight ratio, well below that induced by TAC (Figure 1A). Myocardial DEA/NO-induced sGC activity was nearly 90% lower in Cav3KO versus WT (Figure 5A), whereas the BAY 60–2770 response was identical between groups (Figure 5A). This appeared similar to what we observed with TAC, and supports greater sGC oxidation in the absence of a Cav3-microdomain pool. There was a trend toward reduced protein expression of sGCα_1 in Cav3KO ($P=0.052$), whereas sGCβ1 was unchanged over controls (Figure 5B). However, as the BAY 60–2770 response was similar between groups, total sGC heterodimer probably was unaltered. We next examined sGC activity in membrane microdomains, using the same fractions F4/F5 versus F11 to define the 2 compartments. The DEA/NO response was much less in Cav3KO over WT in the F4/F5 fraction (Figure 5B), whereas both responses were lower but equal in the F11 (NLR) fraction. Interestingly, the response to BAY 60–2770 was also reduced in Cav3KO F4/F5 fractions, whereas in the F11 NLR fraction, it was higher (as in controls and TAC) and similar to littermate controls. The marked decline in the BAY 60–2770 response in F4/F5 fractions in Cav3KO was not due to an absence of sGC in this microdomain, as Western blots of sucrose density gradient fractions (Figure 5D) revealed the presence of each subunit in both microdomains (F4/F5 and F11). This suggests that Cav3 provides an important facilitating function to NO/heme-dependent and independent sGC activation.

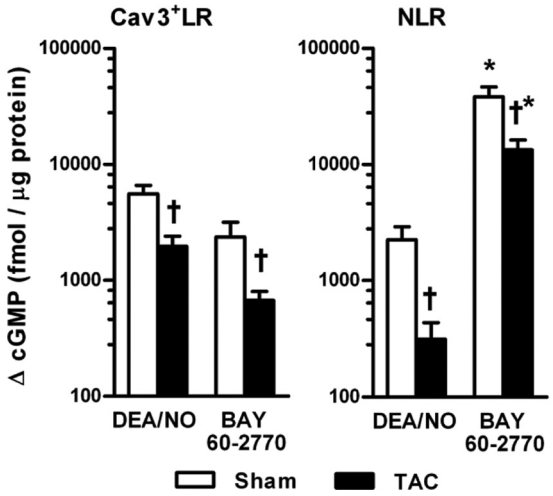

Figure 4. Activation of sGC by NO-donor DEA/NO and NO- and heme-independent sGC activator BAY 60–2770 in Cav3$^+$LR and NLR fractions of sham and TAC hearts. DEA/NO: n=7 for sham, 6 for TAC. BAY 60–2770 n=4 per group: *$P<0.0003$ versus respective DEA/NO; †$P<0.05$ versus respective sham in Cav3$^+$LR; $P<0.03$ versus respective sham in NLR.

Discussion

This study investigated whether and how the activation of myocardial soluble guanylyl cyclase is affected by pressure-overload–induced cardiac hypertrophy. The results highlight several novel and important findings. First, sGC is profoundly modified in the hypertrophied heart, rendering it less NO-responsive yet equally activated by the NO- and heme-independent agonist BAY 60–2770 as compared with controls. This supports the presence of oxidation of sGC, which, though previously documented in the pulmonary and systemic hypertension,[29,30] has not been previously reported in the myocardium. Second, we reveal the presence of a substantial proportion of myocardial sGC in the plasma membrane within microdomains that confer differential activation properties in the normal heart. Specifically, sGC within Cav3-enriched microdomains is more responsive to NO activation and relatively protected from oxidation. By contrast, sGC in nonlipid raft (non-Cav3 containing) domains is less NO responsive and more oxidized. Caveolae-localization of sGC as a mechanism to augment NO responsiveness is consistent with prior work showing colocalization of sGC with NOS3 and PKG[19,20] and NO-cGMP signaling within plasmalemmal caveolae. Third, we link the 2 behaviors, showing that this submembrane distribution of sGC is dynamic, being diminished in Cav3$^+$LR domains by pressure overload, resulting in a shift from NO to BAY 60–2770 sGC-responsiveness. Thus, although heme-oxidation contributes to the overall decline of NO activation of sGC in the hypertrophied heart, this modulation occurs predominantly in noncaveolae enriched microdomains. Last, we show that the presence of Cav3 within lipid rafts is an important regulator of both NO/heme-dependent and heme-independent sGC activation. Viewed together, these observations shed new light on how abnormal subcellular distribution and oxidation of sGC can contribute to depressed cGMP-related signaling in cardiac disease.

Table 2. Differential sGC Responsiveness Within Microdomains of Normal and Hypertrophied Hearts

	Cav3$^+$LR		NLR	
Relative Response	Sham	TAC	Sham	TAC
BAY 60–2770:DEA/NO	1.0	0.6	3.5	17.4

Relative response ratios were calculated using the percent change in cGMP levels within respective microdomains of sham and TAC hearts. Values are normalized to the response ratio of sham Cav3$^+$LR fraction. Increasing BAY 60–2770:DEA/NO ratios reflect enhanced response to BAY 60–2770 and diminished response to DEA/NO, resulting from heme-oxidization of sGC.

Despite its name and differentiation from particulate GC coupled to natriuretic receptors, soluble GC is also detectable in membrane fractions. The $\alpha_2\beta_1$ sGC isoform is found in placenta, epithelia, and neurons and has been shown in rat neuronal synaptic membrane.[21] The $\alpha_1\beta_1$ heterodimer is more ubiquitously expressed,[34] and is also detected in the plasmalemma of vascular endothelial cells,[19] platelets,[19] neuroblastoma cells,[39] and sarcolemma of skeletal,[22,23] smooth,[40] and cardiac muscle tissue.[18,19] The specific function of membrane-associated versus cytosolic sGC$\alpha_1\beta_1$ has been relatively little studied. Zabel et al[19] first identified a translocation of sGC to caveolin-enriched domains in endothelial cells when NO synthesis was stimulated by calcium, and this in turn enhanced cGMP-generation. Castro et al also observed an NO-sGC-cGMP signal in cardiomyocyte subplasmalemma by expressing an olfactory cyclic nucleotide gated membrane channel, though this was considered the particulate (eg, NP-coupled) GC,[41] and not sGC. Other studies have revealed compartmentalized NO-stimulated sGC-cGMP pools that blunt β-adrenergic stimulation modulated by PDE5a,[42] PDE2,[43] and β3-adrenergic signaling,[43,44] suggesting colocalization at the plasma membrane. Whether this functional compartment includes sGC has not been tested. In another study, bovine tracheal smooth muscle showed membrane-associated sGC$\alpha_1\beta_1$ produces the first of 2 sequential cGMP signals involved in muscarinic activation, involving sGC translocation from cytosol to the plasma membrane.[40] How sGC moves remains unclear, though it is found in a complex with NOS3 and heat shock protein 90 (HSP90)[45] and HSP90 can act as a migration chaperone. Clarification of this mechanism awaits further investigation.

The present study is the first to identify differential NO/heme-dependent and heme-independent activation properties of sGC localized within or external to Cav3$^+$LR microdomains. Strikingly, although sGC heme-oxidation appears prevalent in the NLR fraction with TAC, this appears not the case in Cav3$^+$LR. The cause for an apparent protection against oxidation of sGC in the Cav3$^+$LR versus greater oxidation in NLR domains remains unknown. Interestingly, superoxide dismutase 1 has been reported to localize to caveolae in vascular endothelial cells[46] and may confer targeted antioxidant effects. Another study found thioredoxin reductase 1 binds to caveolin-1,[47] though in this instance the interaction was suggested to impede rather than enhance antioxidant activity. As NOS is also localized to this microdomain and can be the target of oxidation depressing its function,[13] it seems plausible that a protected Cav3$^+$LR microdomain would facilitate NO-sGC interaction and cGMP

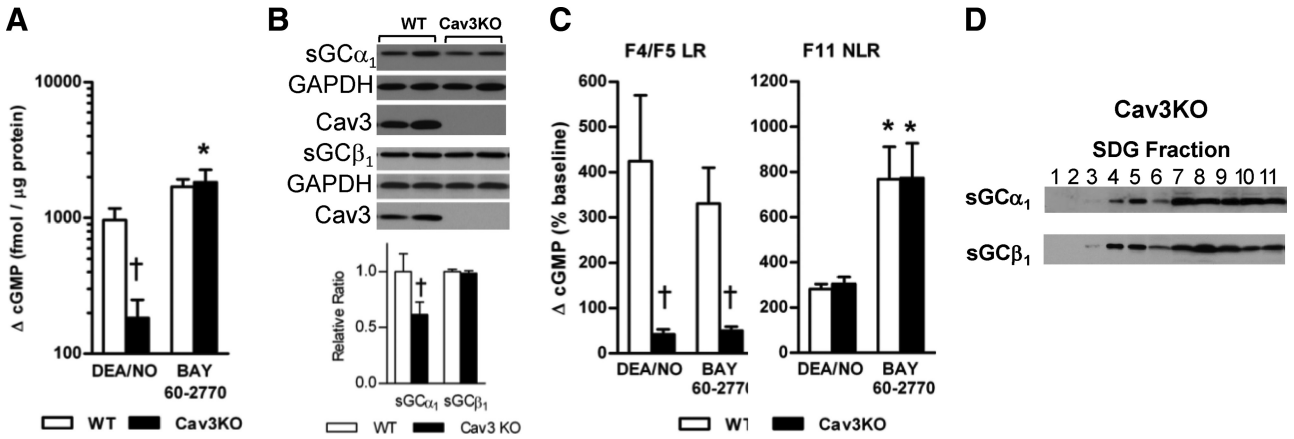

Figure 5. NO-inducible sGC activity is blunted in Cav3KO hearts. A, sGC activation by DEA/NO and BAY 60–2770 in total LV protein of WT and Cav3KO (DEA/NO, n=10; BAY 60–2770, n=4, per genotype). *$P<0.0001$ versus DEA/NO, †$P<0.003$ versus WT. **B**, Western blots of total LV protein, lower panel with summary data, n=6 per bar. †$P=0.052$ versus WT. **C**, sGC activation in F4/F5 lipid raft (LR) versus F11 (NLR) fractions (n=4 per drug, per genotype). *$P<0.05$ versus DEA/NO, †$P<0.04$ versus WT. **D**, Representative Western blot of Cav3KO sucrose density gradient (SDG) fractions.

generation, as we observed. The Cav3KO results further suggest that Cav3 itself plays an important role to this preservation, whether heme/NO dependent or not. The latter may relate to a structural organization of the proteins within caveolae, which become disrupted by elimination of Cav3. Cav3KO mice develop mild cardiac hypertrophy, LV dilatation, and reduced systolic function,[38] whereas cardiac-specific overexpression of Cav3 attenuates pressure-overload hypertrophy,[48] both supporting a cardioprotective role of Cav3. Whether other members of the caveolae subproteome also change with chronic cardiac stress (or perhaps aging) remains unknown but raises an intriguing possibility in the context of abnormal signal transduction in various forms of cardiac hypertrophy and disease.

The exact stoichiometry of sGC subunits in the myocyte microdomains remains unknown, and this is nontrivial to quantify given the isolation procedures involved. Furthermore, we recognize that expression of each isoform does not determine their net balance in a heterodimer, and that this balance may itself alter activation. The shift of β_1 more than α_1 from the Cav3-microdomain suggests that some change in heterodimer composition may have occurred. In the rat brain, postnatal development has been associated with decreased sGC activity despite unaltered sGC subunit expression, and for the cerebrum, this has correlated with less $sGC\alpha_1\beta_1$ heterodimerization.[49] In the human heart, $sGC\alpha_1$ gene expression is nearly 3-fold higher than $sGC\beta_1$ ($sGC\alpha_2$ is undetectable).[34] Our findings support this, suggesting $sGC\beta_1$ may determine sGC NO-responsiveness through heterodimerization with a relative surplus of the α_1 subunit.

Pressure overload has been previously shown to depress NOS activity through functional uncoupling[13] and to augment phosphodiesterase-mediated cGMP hydrolysis.[9] Based on the current data, pressure-overload also results in sGC oxidation and disrupted localization away from $Cav3^+$LR microdomains—further depressing NO-stimulated responsiveness. Each mechanism can play a role in reducing effective cGMP signaling and thus contribute to cardiac stress maladaptations. Because we cannot yet directly manipulate sGC membrane translocation, its in vivo effects on cardiac stress responses admittedly remain speculative. The new results do not conflict with prior observed benefits from PDE5 or PDE1 inhibition[9,50] or from reversing NOS uncoupling by tetrahydrobiopterin (BH4).[51] In the former case, the effect was due to enhancing cGMP once generated, which in turn increased PKG activity. By contrast, BH4 reduced NOS-derived ROS and enhanced NO synthesis, but this did not lead to increased PKG activation. It is possible that persistent sGC dysfunction contributed to this observation. Further studies will be required to test whether reverse remodeling of the hypertrophied heart can restore normal sGC NO sensitivity and relocalize it to $Cav3^+$LR. The present results should help frame such research by highlighting a new sGC regulatory mechanism and providing insights into the potential utility of heme-independent sGC activators for the treatment of heart disease.

Acknowledgments

We thank Gabriela Hernandez, Suruchi Bhardwaj, and David Harris for technical assistance; Johanne-Peter Stasch for providing the BAY compound; and Victor Rizzo for careful reading of the manuscript.

Sources of Funding

This work was supported, in part, by National Heart, Lung, and Blood Institute grants T32-HL007227 (to E.J.T.) and HL093432 (to E.T.); Temple University School of Medicine, Department of Medicine, Faculty Development Research Award (to E.J.T.); and NHLBI grants HL-089297 and HL-093432, Fondation Leducq TransAtlantic Network, the Peter Belfer Laboratory, and the Abraham and Virginia Weiss Professorship (to D.A.K.).

Disclosures

None.

References

1. Guazzi M, Samaja M, Arena R, Vicenzi M, Guazzi MD. Long-term use of sildenafil in the therapeutic management of heart failure. *J Am Coll Cardiol*. 2007;50:2136–2144.
2. Lewis GD, Shah R, Shahzad K, Camuso JM, Pappagianopoulos PP, Hung J, Tawakol A, Gerszten RE, Systrom DM, Bloch KD, Semigran MJ. Sildenafil improves exercise capacity and quality of life in patients with systolic heart failure and secondary pulmonary hypertension. *Circulation*. 2007;116:1555–1562.

3. Lapp H, Mitrovic V, Franz N, Heuer H, Buerke M, Wolfertz J, Mueck W, Unger S, Wensing G, Frey R. Cinaciguat (Bay 58-2667) improves cardiopulmonary hemodynamics in patients with acute decompensated heart failure. *Circulation*. 2009;119:2781–2788.
4. Kinugawa KI, Kohmoto O, Yao A, Serizawa T, Takahashi T. Cardiac inducible nitric oxide synthase negatively modulates myocardial function in cultured rat myocytes. *Am J Physiol*. 1997;272:H35–H47.
5. Kojda G, Kottenberg K, Nix P, Schluter KD, Piper HM, Noack E. Low increase in cGMP induced by organic nitrates and nitrovasodilators improves contractile response of rat ventricular myocytes. *Circ Res*. 1996;78:91–101.
6. Lohmann SM, Fischmeister R, Walter U. Signal transduction by cGMP in heart. *Basic Res Cardiol*. 1991;86:503–514.
7. Mohan P, Brutsaert DL, Paulus WJ, Sys SU. Myocardial contractile response to nitric oxide and cGMP. *Circulation*. 1996;93:1223–1229.
8. Shah AM, Spurgeon HA, Sollott SJ, Talo A, Lakatta EG. 8-bromo-cGMP reduces the myofilament response to Ca^{2+} in intact cardiac myocytes. *Circ Res*. 1994;74:970–978.
9. Takimoto E, Champion HC, Li M, Belardi D, Ren S, Rodriguez ER, Bedja D, Gabrielson KL, Wang Y, Kass DA. Chronic inhibition of cyclic GMP phosphodiesterase 5a prevents and reverses cardiac hypertrophy. *Nat Med*. 2005;11:214–222.
10. Tatsumi T, Matoba S, Kawahara A, Keira N, Shiraishi J, Akashi K, Kobara M, Tanaka T, Katamura M, Nakagawa C, Ohta B, Shirayama T, Takeda K, Asayama J, Fliss H, Nakagawa M. Cytokine-induced nitric oxide production inhibits mitochondrial energy production and impairs contractile function in rat cardiac myocytes. *J Am Coll Cardiol*. 2000; 35:1338–1346.
11. Wegener JW, Nawrath H, Wolfsgruber W, Kuhbandner S, Werner C, Hofmann F, Feil R. cGMP-dependent protein kinase I mediates the negative inotropic effect of cGMP in the murine myocardium. *Circ Res*. 2002;90:18–20.
12. Bayraktutan U, Yang ZK, Shah AM. Selective dysregulation of nitric oxide synthase type 3 in cardiac myocytes but not coronary microvascular endothelial cells of spontaneously hypertensive rat. *Cardiovasc Res*. 1998;38:719–726.
13. Takimoto E, Champion HC, Li M, Ren S, Rodriguez ER, Tavazzi B, Lazzarino G, Paolocci N, Gabrielson KL, Wang Y, Kass DA. Oxidant stress from nitric oxide synthase-3 uncoupling stimulates cardiac pathologic remodeling from chronic pressure load. *J Clin Invest*. 2005; 115:1221–1231.
14. Ecker T, Gobel C, Hullin R, Rettig R, Seitz G, Hofmann F. Decreased cardiac concentration of cGMP kinase in hypertensive animals: an index for cardiac vascularization? *Circ Res*. 1989;65:1361–1369.
15. Nagendran J, Archer SL, Soliman D, Gurtu V, Moudgil R, Haromy A, St Aubin C, Webster L, Rebeyka IM, Ross DB, Light PE, Dyck JR, Michelakis ED. Phosphodiesterase type 5 is highly expressed in the hypertrophied human right ventricle, and acute inhibition of phosphodiesterase type 5 improves contractility. *Circulation*. 2007;116:238–248.
16. Pokreisz P, Vandenwijngaert S, Bito V, Van den Bergh A, Lenaerts I, Busch C, Marsboom G, Gheysens O, Vermeersch P, Biesmans L, Liu X, Gillijns H, Pellens M, Van Lommel A, Buys E, Schoonjans L, Vanhaecke J, Verbeken E, Sipido K, Herijgers P, Bloch KD, Janssens SP. Ventricular phosphodiesterase-5 expression is increased in patients with advanced heart failure and contributes to adverse ventricular remodeling after myocardial infarction in mice. *Circulation*. 2009;119:408–416.
17. Castro LR, Verde I, Cooper DM, Fischmeister R. Cyclic guanosine monophosphate compartmentation in rat cardiac myocytes. *Circulation*. 2006;113:2221–2228.
18. Mery PF, Pavoine C, Belhassen L, Pecker F, Fischmeister R. Nitric oxide regulates cardiac Ca^{2+} current: involvement of cGMP-inhibited and cGMP-stimulated phosphodiesterases through guanylyl cyclase activation. *J Biol Chem*. 1993;268:26286–26295.
19. Zabel U, Kleinschnitz C, Oh P, Nedvetsky P, Smolenski A, Muller H, Kronich P, Kugler P, Walter U, Schnitzer JE, Schmidt HH. Calcium-dependent membrane association sensitizes soluble guanylyl cyclase to nitric oxide. *Nat Cell Biol*. 2002;4:307–311.
20. Linder AE, McCluskey LP, Cole KR III, Lanning KM, Webb RC. Dynamic association of nitric oxide downstream signaling molecules with endothelial caveolin-1 in rat aorta. *J Pharmacol Exp Ther*. 2005; 314:9–15.
21. Russwurm M, Wittau N, Koesling D. Guanylyl cyclase/psd-95 interaction: targeting of the nitric oxide-sensitive alpha2beta1 guanylyl cyclase to synaptic membranes. *J Biol Chem*. 2001;276:44647–44652.
22. Feussner M, Richter H, Baum O, Gossrau R. Association of soluble guanylate cyclase with the sarcolemma of mammalian skeletal muscle fibers. *Acta Histochem*. 2001;103:265–277.
23. Schoser BG, Behrends S. Soluble guanylyl cyclase is localized at the neuromuscular junction in human skeletal muscle. *Neuroreport*. 2001;12: 979–981.
24. Galbiati F, Engelman JA, Volonte D, Zhang XL, Minetti C, Li M, Hou H Jr, Kneitz B, Edelmann W, Lisanti MP. Caveolin-3 null mice show a loss of caveolae, changes in the microdomain distribution of the dystrophin-glycoprotein complex, and t-tubule abnormalities. *J Biol Chem*. 2001; 276:21425–21433.
25. Capozza F, Combs TP, Cohen AW, Cho YR, Park SY, Schubert W, Williams TM, Brasaemle DL, Jelicks LA, Scherer PE, Kim JK, Lisanti MP. Caveolin-3 knockout mice show increased adiposity and whole body insulin resistance, with ligand-induced insulin receptor instability in skeletal muscle. *Am J Physiol Cell Physiol*. 2005;288:C1317–C1331.
26. Takimoto E, Koitabashi N, Hsu S, Ketner EA, Zhang M, Nagayama T, Bedja D, Gabrielson KL, Blanton R, Siderovski DP, Mendelsohn ME, Kass DA. Regulator of g protein signaling 2 mediates cardiac compensation to pressure overload and antihypertrophic effects of pde5 inhibition in mice. *J Clin Invest*. 2009;119:408–420.
27. Hesketh GG, Shah MH, Halperin VL, Cooke CA, Akar FG, Yen TE, Kass DA, Machamer CE, Van Eyk JE, Tomaselli GF. Ultrastructure and regulation of lateralized connexin43 in the failing heart. *Circ Res*. 2010; 106:1153–1163.
28. Nagayama T, Hsu S, Zhang M, Koitabashi N, Bedja D, Gabrielson KL, Takimoto E, Kass DA. Pressure-overload magnitude-dependence of the anti-hypertrophic efficacy of pde5a inhibition. *J Mol Cell Cardiol*. 2009; 46:560–567.
29. Stasch JP, Schmidt PM, Nedvetsky PI, Nedvetskaya TY, H SA, Meurer S, Deile M, Taye A, Knorr A, Lapp H, Muller H, Turgay Y, Rothkegel C, Tersteegen A, Kemp-Harper B, Muller-Esterl W, Schmidt HH. Targeting the heme-oxidized nitric oxide receptor for selective vasodilatation of diseased blood vessels. *J Clin Invest*. 2006;116:2552–2561.
30. Pankey EA, Bhartiya M, Badejo AM Jr, Haider U, Stasch JP, Murthy SN, Nossaman BD, Kadowitz PJ. Pulmonary and systemic vasodilator responses to the soluble guanylyl cyclase activator, bay 60–2770, are not dependent on endogenous nitric oxide or reduced heme. *Am J Physiol Heart Circ Physiol*. 2011;300:H792–H802.
31. Friebe A, Mergia E, Dangel O, Lange A, Koesling D. Fatal gastrointestinal obstruction and hypertension in mice lacking nitric oxide-sensitive guanylyl cyclase. *Proc Natl Acad Sci U S A*. 2007;104: 7699–7704.
32. Friebe A, Wedel B, Harteneck C, Foerster J, Schultz G, Koesling D. Functions of conserved cysteines of soluble guanylyl cyclase. *Biochemistry*. 1997;36:1194–1198.
33. Wedel B, Humbert P, Harteneck C, Foerster J, Malkewitz J, Bohme E, Schultz G, Koesling D. Mutation of his-105 in the beta 1 subunit yields a nitric oxide-insensitive form of soluble guanylyl cyclase. *Proc Natl Acad Sci U S A*. 1994;91:2592–2596.
34. Budworth J, Meillerais S, Charles I, Powell K. Tissue distribution of the human soluble guanylate cyclases. *Biochem Biophys Res Commun*. 1999; 263:696–701.
35. Mergia E, Friebe A, Dangel O, Russwurm M, Koesling D. Spare guanylyl cyclase NO receptors ensure high NO sensitivity in the vascular system. *J Clin Invest*. 2006;116:1731–1737.
36. Koesling D, Herz J, Gausepohl H, Niroomand F, Hinsch KD, Mulsch A, Bohme E, Schultz G, Frank R. The primary structure of the 70 kDa subunit of bovine soluble guanylate cyclase. *FEBS Lett*. 1988;239:29–34.
37. Knorr A, Hirth-Dietrich C, Alonso-Alija C, Harter M, Hahn M, Keim Y, Wunder F, Stasch JP. Nitric oxide-independent activation of soluble guanylate cyclase by bay 60–2770 in experimental liver fibrosis. *Arzneimittelforschung*. 2008;58:71–80.
38. Woodman SE, Park DS, Cohen AW, Cheung MW, Chandra M, Shirani J, Tang B, Jelicks LA, Kitsis RN, Christ GJ, Factor SM, Tanowitz HB, Lisanti MP. Caveolin-3 knock-out mice develop a progressive cardiomyopathy and show hyperactivation of the p42/44 mapk cascade. *J Biol Chem*. 2002;277:38988–38997.
39. Jones JD, Carney ST, Vrana KE, Norford DC, Howlett AC. Cannabinoid receptor-mediated translocation of no-sensitive guanylyl cyclase and production of cyclic GMP in neuronal cells. *Neuropharmacology*. 2008;54: 23–30.
40. Uray FP, Alfonzo RG, de Becemberg IL, Alfonzo MJ. Muscarinic agonists acting through m2 acetylcholine receptors stimulate the migration of an NO-sensitive guanylyl cyclase to the plasma membrane

of bovine tracheal smooth muscle. *J Recept Signal Transduct Res.* 2009; 30:10–23.
41. Castro LR, Schittl J, Fischmeister R. Feedback control through cGMP-dependent protein kinase contributes to differential regulation and compartmentation of cGMP in rat cardiac myocytes. *Circ Res*. 2010;107: 1232–1240.
42. Takimoto E, Belardi D, Tocchetti CG, Vahebi S, Cormaci G, Ketner EA, Moens AL, Champion HC, Kass DA. Compartmentalization of cardiac beta-adrenergic inotropy modulation by phosphodiesterase type 5. *Circulation*. 2007;115:2159–2167.
43. Mongillo M, Tocchetti CG, Terrin A, Lissandron V, Cheung YF, Dostmann WR, Pozzan T, Kass DA, Paolocci N, Houslay MD, Zaccolo M. Compartmentalized phosphodiesterase-2 activity blunts beta-adrenergic cardiac inotropy via an NO/cGMP-dependent pathway. *Circ Res*. 2006;98:226–234.
44. Lee DI, Vahebi S, Tocchetti CG, Barouch LA, Solaro RJ, Takimoto E, Kass DA. PDE5a suppression of acute beta-adrenergic activation requires modulation of myocyte beta-3 signaling coupled to PKG-mediated troponin I phosphorylation. *Basic Res Cardiol*. 2010;105:337–347.
45. Venema RC, Venema VJ, Ju H, Harris MB, Snead C, Jilling T, Dimitropoulou C, Maragoudakis ME, Catravas JD. Novel complexes of guanylate cyclase with heat shock protein 90 and nitric oxide synthase. *Am J Physiol Heart Circ Physiol*. 2003;285:H669–H678.
46. van der Loo B, Bachschmid M, Skepper JN, Labugger R, Schildknecht S, Hahn R, Mussig E, Gygi D, Luscher TF. Age-associated cellular relocation of sod 1 as a self-defense is a futile mechanism to prevent vascular aging. *Biochem Biophys Res Commun*. 2006;344:972–980.
47. Volonte D, Galbiati F. Inhibition of thioredoxin reductase 1 by caveolin 1 promotes stress-induced premature senescence. *EMBO Rep*. 2009;10: 1334–1340.
48. Horikawa YT, Panneerselvam M, Kawaraguchi Y, Tsutsumi YM, Ali SS, Balijepalli RC, Murray F, Head BP, Niesman IR, Rieg T, Vallon V, Insel PA, Patel HH, Roth DM. Cardiac-specific overexpression of caveolin-3 attenuates cardiac hypertrophy and increases natriuretic peptide expression and signaling. *J Am Coll Cardiol*. 2011;57:2273–2283.
49. Haase N, Haase T, Seeanner M, Behrends S. Nitric oxide sensitive guanylyl cyclase activity decreases during cerebral postnatal development because of a reduction in heterodimerization. *J Neurochem*. 2010;112: 542–551.
50. Jeon KI, Jono H, Miller CL, Cai Y, Lim S, Liu X, Gao P, Abe J, Li JD, Yan C. Ca^{2+}/calmodulin-stimulated PDE1 regulates the beta-catenin/TCF signaling through pp2a b56 gamma subunit in proliferating vascular smooth muscle cells. *FEBS J*. 2010;277:5026–5039.
51. Moens AL, Takimoto E, Tocchetti CG, Chakir K, Bedja D, Cormaci G, Ketner EA, Majmudar M, Gabrielson K, Halushka MK, Mitchell JB, Biswal S, Channon KM, Wolin MS, Alp NJ, Paolocci N, Champion HC, Kass DA. Reversal of cardiac hypertrophy and fibrosis from pressure overload by tetrahydrobiopterin: efficacy of recoupling nitric oxide synthase as a therapeutic strategy. *Circulation*. 2008;117:2626–2636.

Novelty and Significance

What Is Known?

- Nitric oxide (NO) stimulates the conversion of guanosine triphosphate to cyclic guanosine monophosphate (cGMP) by soluble guanylyl cyclase (sGC). cGMP regulates a wide spectrum of cardiovascular processes including cardiac contractility and chronic cardiac hypertrophy.
- Cardiovascular disease depresses sGC activity, however, the mechanism of this reduction in cyclase activity is poorly understood.

What New Information Does This Article Contribute?

- Pressure-overload cardiac stress results in the oxidation of myocardial sGC, rendering it less responsive to NO in the hypertrophied heart.
- sGC within caveolae-enriched membrane microdomains of both normal and hypertrophied hearts is relatively protected from oxidation, demonstrating enhanced NO-responsiveness relative to sGC within noncaveolae-enriched microdomains.
- Submyocardial distribution of sGC is dynamic. Pressure-overload cardiac stress induces a relocalization of the membrane associated sGC away from caveolae.
- Caveolin 3 itself is important for the NO responsiveness of sGC. Deletion of caveolin 3 reduces sGC NO- and heme-independent activation in lipid-raft domains.

Reduced NO-cGMP signaling contributes to the pathophysiology of cardiovascular disease. This has been attributed to depressed NO synthase activity through functional uncoupling and to diminished cGMP signaling due to augmented phosphodiesterase-mediated cGMP hydrolysis. In pulmonary and systemic hypertension, oxidation of sGC depresses cyclase activity; thereby further diminishing cGMP signaling. We provide evidence that sGC activity is markedly reduced in pressure-overload hypertrophied myocardium not due to reduced expression but rather to oxidation that suppresses both NO and heme-dependent activity. We found that both cyclase oxidation and its NO-activation are differentially impacted depending on the subcellular membrane localization of sGC. sGC is found in both cytosol and membrane at near equal levels. When residing in caveolae-enriched membrane lipid rafts, sGC is more responsive to NO-activation and relatively protected from oxidation as compared with sGC in nonlipid raft domains. Pressure overload triggers a relocalization of sGC out of caveolae-enriched lipid rafts to nonlipid rafts, and this reduces NO responsiveness while increasing enzyme oxidation Furthermore, caveolin-3 regulates both NO/heme-dependent and NO/heme-independent sGC activation in lipid rafts. These findings link dynamic subcellular localization with differential enzyme oxidation and activity, revealing a novel regulatory mechanism of sGC activity. Our work also suggests the caveolae microdomain as a potential therapeutic target for cardiac hypertrophy and heart failure.

SUPPLEMENTAL MATERIAL

Methods.

Pressure Overload Model

Mice were anesthetized with isoflurane (3%–4%, inhaled) and etomidate (0.3mg, i.m. injection), intubated, and mechanically ventilated. The transverse aorta was constricted with a 27-gauge needle using 7-0 prolene suture, after which the chest was closed and the animal allowed to recover from anesthesia. Sham control mice were subjected to thoracotomy alone. All animals were studied at 3 wk after surgery. All animals received humane care according to NIH guidelines, and all animal protocols were approved by the respective IACUCs of Johns Hopkins University and Temple University.

Immunohistochemistry analysis of myocardium

Mounted LV tissue slices were dually immunostained with either rabbit anti-sGCα_1 (1:100, Abcam) or rabbit anti-sGCβ_1 (1:100, Cayman Chemicals) and mouse anti-Cav-3 (1:200, BD Transduction Laboratories) primary antibodies. Anti-mouse Alexa 594 (1:100, Molecular Probes) and anti-rabbit Alexa 488 (1:100, Molecular Probes) secondary antibodies were used. Tissue slices were also stained with diluted DAPI solution.

Mounted LV tissue slices were deparaffinized, processed for antigen retrieval, and blocked with 1% BSA/PBST for 30 min at room temperature and then with 20mg/ml Mouse Antibody Fragment Fab (goat anti-mouse 10ug/ml, Vector Lab) in 1% BSA/PBST for 1 h at room temperature. Mounted tissue slices were then incubated with either rabbit anti-sGCα_1 (1:100, Abcam) or rabbit anti-sGCβ_1 (1:100, Cayman Chemicals) primary antibody in 1%BSA/PBST in a humidified chamber overnight at 4°C, washed, incubated with anti-rabbit Alexa 488 (1:100, Molecular Probes) secondary antibody in 1% BSA/PBST for 4 h at room temperature in the dark, and then washed and blocked a second time with 1% BSA/PBST for 30 min at room temperature in the dark. Mounted LV tissue slices were then incubated with the second primary antibody, mouse anti-Cav-3 (1:200, BD Transduction Laboratories), in 1% BSA/PBST in a humidified chamber in the dark at 4°C overnight, washed, incubated with anti-mouse Alexa 594 secondary antibody (1:100, Molecular Probes) in 1% BSA/PBST for 1 h at room temperature in the dark. Mounted LV tissue was washed well with PBS, briefly stained with diluted DAPI solution, washed again, and then sealed with a cover slip.

Cell and Membrane Fractionation

Tissue homogenization was carried out in detergent free buffer of 50mM Tris-HCl, pH 7.6, 1mmol/L EDTA, 1mmol/L DTT, and 2mmol/L PMSF(59). Following sucrose density gradient ultracentrifugation of the sample, fractions were collected every 400 µl from the top sucrose layer, corresponding to F1 (top, most buoyant) to F11 (bottom, least buoyant, heaviest). A light-scattering band confined to the 35–5% sucrose interface, F4-F5, corresponds to Cav3$^+$LR fractions. Proteins were precipitated using 0.1% w/v deoxycholic acid in 100% w/v trichloroacetic acid. Protein concentrations were determined by Bradford assay. Non-lipid raft (NLR, F11) and Cav3$^+$LR fractions (F4 and F5) without TCA precipitation were also collected for Bradford and subsequent cGMP assays.

To prepare membrane-cytosol fractions, LV tissue samples were homogenized in a sucrose buffer (10 mmol/L imidazole, 300 mmol/L sucrose, 10 mmol/L NaF, 1 mmol/L EDTA) with protease inhibitors (0.3 mmol/L PMSF, 0.5 mmol/L DTT, 10 µg/ml aprotinin, 10 µg/ml leupeptin, 2 µg/ml pepstatin A) and centrifuged briefly at 2,000*g* to pellet the nuclear/indestructible cell fraction. The resulting supernatant was centrifuged at 20,000*g* for 1 h, and the final supernatant kept as the cytosolic fraction. The pellet was resuspended in high-salt buffer (25 mmol/L Tris pH 7.4, 500 mmol/L NaCL, 1 mmol/L EDTA, 1 mmol/L EGTA + protease inhibitors) incubated for 30 min, and centrifuged at 16,000*g* for 10 min. The pellet was resuspended in the same high-salt buffer with 0.5% Triton, incubated for 30 min, re-centrifuged at 16,000*g* for 10 min, and the

resulting supernatant collected as the membrane fraction. Protein concentrations were measured by BCA assay (Pierce).

Isolation of caveolin-enriched lipid raft fraction.

LV tissue homogenization was carried out on ice, in detergent free buffer (50 mmol/L Tris-HCl, pH 7.6, 1 mmol/L EDTA, 1 mmol/L DTT, 2 mmol/L PMSF, 50mmol/L NaF, 1mmol/L Na Vanadate) with protease inhibitors (Mammalian Cocktail, Sigma-Aldrich). Following 1 h incubation on ice with intermittent vortex, 0.6mL of tissue homogenate was mixed with 1.4mL of 60% (w/v) sucrose in 20mmol/L KCl, 0.5mmol/L $MgCl_2$ and placed at the bottom of an ultracentrifuge tube. A discontinuous 35%-5% sucrose gradient was formed by overlaying each sample with 1.3mL of 35% sucrose and then with 1.3mL of 5% sucrose. The sucrose density gradient was topped off with 0.5mL of 200mmol/L KCl. Each sample was then centrifuged at >130,000g for 18 h at 4°C in a swinging bucket rotor (Beckman Instruments, Palo Alto, CA) without any brake. The top KCl layer was discarded and fractions were collected every 400 µl from the top sucrose layer corresponding to F1 (top) to F11 (bottom).

Primary Antibody Concentration and Sources for Western Blot

$sGC\alpha_1$ (1:1000, gifted by A. Friebe, also Abcam), $sGC\beta_1$ (1:4000, Cayman Chemicals), Cav-3 (1:10000, BD Transduction), and GAPDH (1:10000, Cell Signaling). Specificity of anti-$sGC\alpha_1$ and -β_1 antibodies were confirmed using protein extracts from sGC $\alpha_1^{-/-}$ and sGC $\beta_1^{-/-}$ mouse hearts (gifted by A. Friebe). Primary antibody binding was visualized by horseradish peroxidase–conjugated secondary antibodies and enhanced chemiluminescence (GE Healthcare).

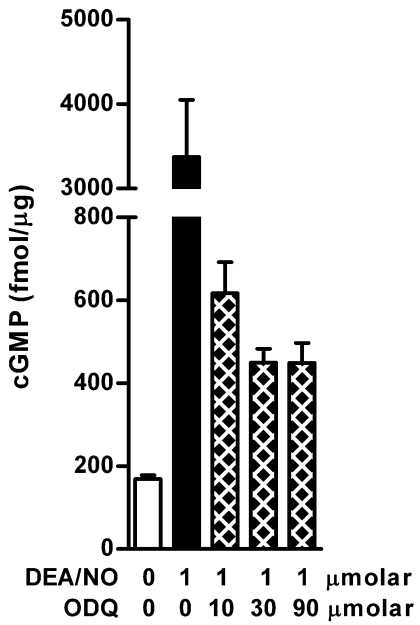

Online Figure I. Titration of sGC inhibitor ODQ. cGMP levels of total protein extract from C57BL/6 LV homogenate were measured by ELISA in the absence and presence of DEA/NO and ODQ at the concentrations indicated. N=4 per condition. * *P*<0.05 versus unstimulated (open bar). ‡ *P*<0.05 versus DEA/NO 1 µmolar without ODQ (black bar).

sGC activity assay

Homogenates were pre-incubated at room temperature for 15 min in a solution for final concentrations of Tris 50mM, pH7.6, IBMX 0.75mmol/L, creatine phosphate 3.5mmol/L, creatinine phosphokinase 1 unit, GTP 1mmol/L, and $MgCl_2$ 3mmol/L. Samples were then incubated with or without DEA/NO (1µmol/L) or BAY 60-2770 (0.1µmol/L) at 37°C for 10 min and and subjected to diethyl ether extraction. cGMP levels of ether-extracted samples were measured by EIA. ODQ (1H-[1,2,4] oxadiazolo[4,3-a]quinoxalin1- one) was used to inhibit sGC as a negative control. BAY compound was provided by J-P Stasch (Bayer AG, Wuppertal, Germany).